Radiation Physics and Chemistry 166 (2020) 108464

Contents lists available at ScienceDirect

Radiation Physics and Chemistry

journal homepage: www.elsevier.com/locate/radphyschem

OSL using a prototype fibre-mounted sensor and automated reader assembly

A.K.M. Mizanur Rahman[a,c], Mahfuza Begum[b,c], H.T. Zubair[c], H.A. Abdul-Rashid[c], Z. Yusoff[c], N.M.Ung[d], D.A. Bradley[e,f,*]

[a] Health Physics Division, Atomic Energy Centre, Bangladesh Atomic Energy Commission, 4 Kazi Nazrul Islam Avenue, Shahbag, Dhaka, 1000, Bangladesh
[b] Health Physics & Radioactive Waste Management Unit, Institute of Nuclear Science and Technology, Atomic Energy Research Establishment, Bangladesh Atomic Energy Commission, Ganakbari, Savar, Dhaka, Bangladesh
[c] Fibre Optics Research Centre, Faculty of Engineering, Multimedia University, Jalan Multimedia, 63100, Cyberjaya, Malaysia
[d] Clinical Oncology Unit, Faculty of Medicine, University of Malaya, 50603, Kuala Lumpur, Malaysia
[e] Department of Physics, University of Surrey, Guildford, GU2 7XH, United Kingdom
[f] Sunway University, Centre for Biomedical Physics, 46150, PJ, Malaysia

ARTICLE INFO

Keywords:
Optically stimulate luminescence
nanoDot OSLD
Prototype OSL reader
Fibre-optic coupled dosimeter

ABSTRACT

Application-viable yields of optically stimulated luminescence (OSL) are known to be provided by a number of materials, Al_2O_3:C nanoDot OSLDs being one of those currently favoured, dominating the world of commercial passive radiation dosimetry. Associated with the use of such materials is the need for versatile, high performance readout devices, opportunities remaining for novel developments in support of the OSL media, as emphasised herein. Present study focuses on the data acquisition capability of an in-house prototype OSL reader, luminescence stimulation being provided by a 30 mW green LED light (spectral mid-point ~ 515 nm). In providing for the additional versatility of making stand-off (at a distance) measurements, the dosimeter sensors (nanoDot OSLD chips) were attached to a polymethyl-methcrylate (PMMA) fibre cable, allowing characterization of the OSL (phosphorescence) at very low risk. Using this prototype instrument, key OSL features from an Al_2O_3:C sensor medium have been captured, excellent quantitative agreement being found between present results and those of others using other readers. One further feature of the current design is that it also allows investigation of the excitation light wavelength dependence of sensor media that could be competitive to Al_2O_3:C, there being the additional ability to swap out the OSL sensor, filters and other support components.

1. Introduction

Dosimetrically useful optically stimulated luminescence (OSL) yields have been reported for a number of irradiated materials, including carbon-doped aluminium-oxide (Al_2O_3:C). The latter is a material that has notably been commercialized by Landaeur Inc USA as the key component of an OSL dosimeter (Yukihara et al., 2014). Indeed, passive optically stimulated dosimeters (OSLDs) have been produced in providing for a range of applications, resulting in a variety of trade names, for example: Luxel$^+$ (a dosimeter badge for personnel monitoring and area monitoring), nanoDot OSLD (for patient dose measurements in medical dosimetry) and InLight Basic (for X, gamma, beta radiation sensing). In recent years beryllium oxide (BeO) has also been determined to be yet another promising candidate OSL dosimetry material, leading to development of commercial BeO-based OSL dosimetry systems (BeOSL from Dosimetrics GmbH Munich and BeOmax from TU Dresden) (Sommer et al., 2011). While all of these are badge-type dosimeter systems, constructed commercially for single point assessments, OSL fibre-mounted sensor arrangements (as herein) have been previously described, an instance being that of Gaza et al. (2005), albeit not resulting in a commercial system.

OSL is conventionally a two-stage process, comprising irradiation of the dosimeter followed by optical stimulation. During irradiation of an OSL material two major phenomena occur: atomic ionization of valence electrons and consequent creation of electron-hole pairs. Defects preexisting within crystalline OSL materials form traps within the forbidden gap (the crystalline model also having been shown to produce useful interpretation of the signal produced by amorphous media, glass-based sensor systems being one such example), localizing electrons and holes. When the irradiated samples are subsequently exposed to light stimuli the situation provides for absorption of energy, the recombination of free electrons with localized holes resulting in radiative (luminescence) emission, allowed transitions occurring from the localized traps into the delocalized conduction band (Yukihara and

* Corresponding author. Department of Physics, University of Surrey, Guildford GU2 7XH, United Kingdom.
E-mail address: d.a.bradley@surrey.ac.uk (D.A. Bradley).

https://doi.org/10.1016/j.radphyschem.2019.108464
Received 24 May 2019; Received in revised form 21 August 2019; Accepted 23 August 2019
Available online 30 August 2019
0969-806X/

McKeever, 2011; Bøtter-Jensen et al., 2003).

In what is to follow, the term OSL is used to indicate the signal observed during optical stimulation (the true OSL signal) while for the signal emitted upon termination of stimulation this is phosphorescence, characterized in detail by Ahmed et al. (2016) for Al_2O_3:C. Emission from the samples occurs over a fairly wide spectral range, with wavelengths short compared to the wavelength of the stimulating source. During stimulation the emitted luminescence from the sample can be detected as a function of time, captured via use of a suitable detector system (an example of which is a combined sensor-photomultiplier tube, PMT, assembly). Commercially, a popular system is the Landauer microSTARii reader used in combination with nanoDots sensors.

One possible stimulation strategy is to illuminate the sample with visible light at constant intensity and to record the OSL signal. The absorbed dose is estimated from integration of the OSL signal over some predetermined time interval. The OSL dose response is influenced by a number of factors, one being the effect on detected intensity and spectral distribution from the optical filter that prefaces the PMT, another being the choice between use of the initial OSL intensity or the integrated OSL signal, namely the true OSL signal plus the phosphorescence (Yukihara et al., 2004). The Al_2O_3:C based nanoDot OSLD is said by its manufacturer to be suitable for multiple use with negligible degradation of signal, depending on stimulus duration time. Clearly, an OSL material that is effective for dosimetry should possess a number of desirable properties, including a high photo-ionization cross section, the existence of defects in the green-blue region and a luminescence emission band lying between 350 and 425 nm. The wavelength is limited by the availability of suitable filters and light sources, also the need for sensitive PMTs or other potential light amplification systems. Sensitive detection requires a good signal to noise ratio, aided by separation of the stimulating wavelength from the emission wavelength (Akselrod et al., 2007; Barve et al., 2013). Through wise choice of device elements together with judicious signal handling the advantages of the OSL technique can include high sensitivity, maximum delivery of light (via an optical waveguide), fast readout time and relatively simple reader equipment. In present studies an in-house assembled prototype OSL reader has been performance-evaluated, as detailed below. The dosimeter sensors (nanoDot OSLD chips) were attached to a polymethyl-methcrylate (PMMA) fibre cable, allowing at a distance characterization of the OSL, offering veratility with a degree of novelty.

2. Materials and methods

2.1. Active probe preparation from nanoDot OSLD

The Al_2O_3:C (effective atomic number 11.28) nanoDot OSLD film is made up of a photosensitive aluminium oxide powder coating on a 0.2 mm thick white polystyrene film roll (Wesolowska et al., 2017). This film is encapsulated inside a water-equivalent light-tight plastic case of Archimedean density 1.03 g/cm^3 (Ponmalar et al., 2017; Yusuf et al., 2017; Kerns et al., 2011). In present work the probes were prepared by separating the film from the case and resizing the circular film-strips from a diameter of 5 mm–2 mm, subsequently locating this on the tip of the PMMA fibre (Super Eska SK-40, Mitsubishi Rayon Co., Ltd, Japan). The active volume of the probe was then covered with opaque Teflon tape, mitigating against any signal depletion due to extraneous light exposure. The detailed diagram of the probe assembly has been given in a previous publication focusing on radioluminescence (RL) measurements (Mizanur Rahman et al., 2018); the same arrangement can be used for OSL evaluations. In providing for RL the need is for a detector medium that in response to irradiation yields a fast rise time as well as a fast return to baseline (obtained in our RL version using Ge-doped and P-doped radiation sensitive tips); high performance timing capability can arise from this. For OSL systems the obverse of a slow return to baseline is required (as provided for example by Al_2O_3:C). Our system allows for interchange of the tips (the sensor), the choice depending on application, RL or OSL. The need for flat/highly polished faces to the probe assembly is of course implied, providing for excellent light transport.

Stimulation in the present reader is effected using a 30 mW green LED light (spectral centre 515 nm). Other than the previously mentioned adaptation for radioluminenescence investigations (Mizanur Rahman et al., 2017, 2018), the system is similar to that of others, comprising a radiation-sensitive tip of Al_2O_3:C, together with a fibre cable in combination with a dichroic mirror and well chosen filters to allow separation of stimulation and emission (see for instance, Aznar, et al., 2004; Klein et al., 2005; Gaza et al., 2005; Klein et al., 2006; Andersen et al., 2009).

To allow stand-off measurements, particular sample dosimeter sensors (nanoDot OSLD chips) can be attached to Polymethyl-methcrylate (PMMA) fibre cable, as herein, providing for characterization of the luminescence signal. The signal has been detected with a PMT with a combined band-pass filter (315–445 nm). Measurements were made 24 h post-irradiation in order to allow for equilibration of the irradiated medium, the stimulating LED source being applied in interrogation of the OSL detector. With this, recording was made of the continuous wave (CW) OSL decay curve as a function of stimulation time. Acknowledging OSL materials to be highly light sensitive, the entire process has been carried out in light-tight situation. The total OSL counts have been calculated via integration of the OSL decay curve, beginning from initiation of stimulation through to several tens of seconds of readout time.

2.2. Prototype reader

As previously indicated, the dominant challenge in building a sensitive OSL reader is selection of the appropriate optics and electronics, needing to be sufficient in performance to allow capture of the relatively weak light signal emitted by the luminescing medium. An important challenge was the need to produce a device within the boundaries of a limited experimental budget, a budget far less than the cost of purchasing a commercially available system. Faced with this challenge, numerous methods were considered in seeking to reduce costs while also increasing flexibility, including the use of off-the-shelf optical components. The heart of the present readout setup is a dichroic mirror (offering a cut-off wavelength of 505 nm); this acts as a reflective filter between the stimulating light and luminescence signal. To capture as much light as possible, the rectangular dichroic mirror (Thorlabs DMLP505R) was fitted in a Cage Cube with a C-mount interchangeable Hamamatsu (A11214) block. The stimulation source, a light-emitting diode (LED), has been operated via a programmable LED driver connected through a USB port. In specific terms, use has been made of a CW green source (centred at 515 nm, maximum output power 30 mW at 1 A). The robust, high brightness, compact LED module has been coupled into a PMMA patch cord (numerical aperture, NA = 0.5) via a fibre-coupled (FC) receptacle. To collect the luminescence signal from the fibre-optic coupled dosimeter (FOCD) and to convert it into an electrical signal, the detection hardware needs to contain optics providing for wavelength discrimination and a suitable photo-detector. In the present case use has been made of a PMT of large aperture (5 mm diameter), with high wavelength sensitivity from 300 nm to 720 nm, together with appropriate data acquisition software interface (Mizanur Rahman et al., 2017). These details are specific to the present arrangement.

2.3. Irradiation setup

To provide for irradiation, use was made of a clinical linear accelerator (Varian 2100C/D) generating a 6 MV X-ray photon beam at a dose-rate of 600 cGy/min at 0° gantry angle. The samples were placed on the central-axis of the radiation field at the position of maximum depth-dose, $D_{\max}$ (1.5 cm) within a phantom of *solid-water^{TM}*, the latter

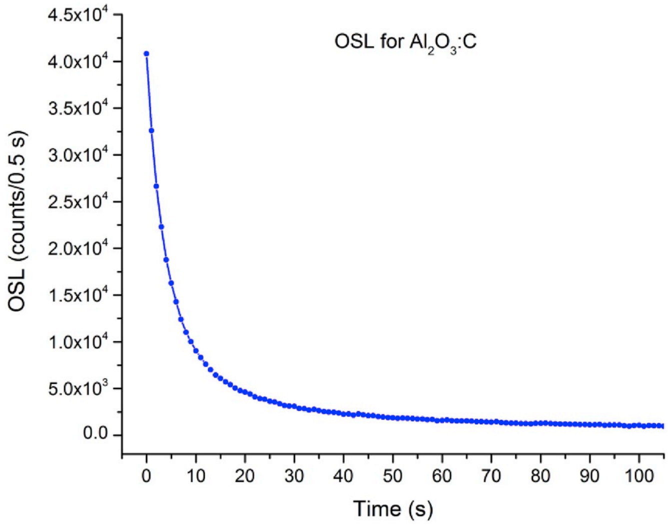

Fig. 1. OSL arising from optical stimulation of Al_2O_3:C post 6 MV X-ray dose delivery of 2 Gy, with stimulation from use of a broad-spectrum wavelength centred at 515 nm.

providing the full scatter conditions conventionally prescribed in MV dosimetry. The source to surface distance was fixed at 100 cm (mitigating against detection of secondary (scattered) electron contamination from the collimator system). The field size was set at (10 × 10) cm^2, also conventional in MV systems dosimetry protocols.

3. Results and discussion

3.1. Luminescence from standard Al_2O_3:C

Fig. 1 results from present use of an Al_2O_3:C sensor irradiated at a dose of 2 Gy delivered by a 6 MV X-ray photon beam. A typical OSL curve is obtained, stimulation being provided at room temperature (22 °C) in the constant wave (CW) green light illumination mode. The first data point was obtained at 800 ms, this and subsequent data points representing the OSL signal integrated over a gate time of 500 ms. Data recording was made for a total time of just over 100 s. In the particular example efficient readout of the stored energy by the sensor has been obtained, the associated uncertainties being of the order of the size of the data points, reflective of the reproducibility, sensitization, precision and accuracy (as discussed in Section 3.2 below). Also apparent is the residual slow phosphorescence signal post optical stimulation. The shape of decay produced by the present fibre-optic coupled dosimeter (FOCD) and readout system assembly is identical with that reported elsewhere for Al_2O_3:C crystals (Yukihara and McKeever, 2011; Granville et al., 2014), the resulting signal decreasing over time in an exponential-like fashion.

In regard to commercial reader systems, eg the microStar reader, compared with the present reader, a point of note is that the former are purposed to meet a specific market demand, namely provision of post-analysis dose results, arising from use of a particular probe (eg Al_2O_3:C). In comparison, the present system offers the ability to swop-out different probes and support components, filters for instance, thus allowing analysis of the OSL and phosphorescence response of particular materials. The resulting information allows for the most appropriate choice of detection window for OSL measurements, encompassing issues of sensitization etc. Here it is important to note that choice should be made of the most suitable optical filter for the PMT, selection being based on the emission spectrum of the dosimetric materials (Marcazzó et al., 2011). This is particularly important given that the intensity of the luminescence signal arising from stimulation is typically many orders of magnitude less than the stimulation light signal. An additional point is the need to guard against use of a stimulation duration that completely depletes all dosimetric traps. With use of short stimulation durations of say less than 1 s, this can be both sufficient in estimating the absorbed dose (Yukihara and McKeever, 2008) as well as preserving a fraction of the radiation-induced trapped charge concentration for subsequent readouts should retrospective evaluations be required.

3.2. Controlled depletion study of the Al_2O_3:C and linked reader assembly

Here interest was in the extent to which measurements could best be controlled using the assembly. In this regard, use was made of the Al_2O_3:C sensor pre-irradiated to a dose of 3 Gy, attached through a 0.5 m length of 1 mm core diameter PMMA fibre to the reader. The choice was made of a 5 s interval between successive stimulations (the LED light-off period), providing for a total of 20 periodic stimulations, each of 800 ms duration. Fig. 2 records the successive and highly reproducible fractional de-trapping, depleting from the initial OSL intensity. In regard to overall precision of measurements, the various influences are acknowledged to include reader stability, controlled through judicious choice of components, dosimeter-dependent factors (eg crystal volume, crystal interfacing with the PMMA), readout protocol and the analytical method. The strong sensitivity results in good part from minimal loss in counts, obtained through careful PMMA-crystal interfacing, a matter also noted by Yukihara and McKeever (2008). Evaluations such as these are of importance, notably allowing prediction of system performance, not least in 'real time' OSL. In this, the OSL procedure involves periodic "pulsing" of the light stimulation at the same time as conduct of periodic irradiation, continuously

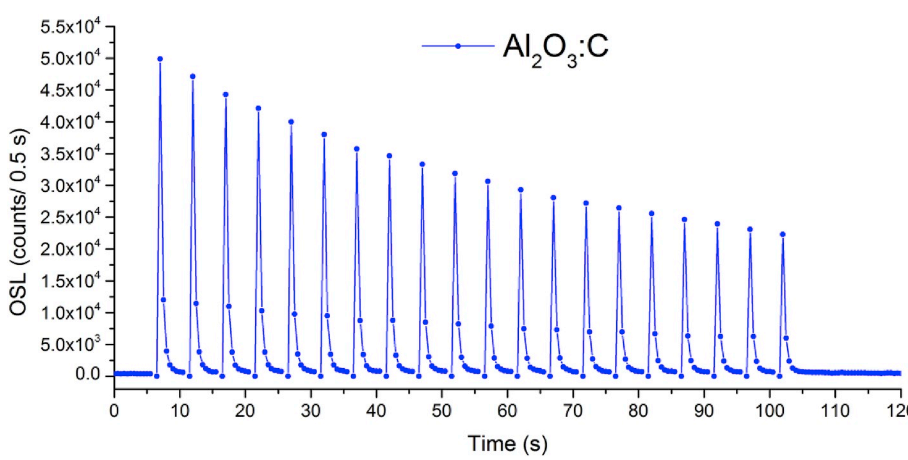

Fig. 2. Controlled depletion study of Al_2O_3:C.

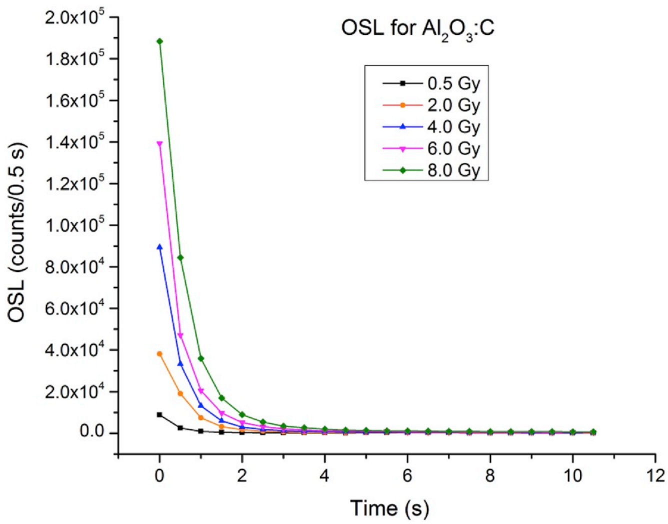

Fig. 3. CW-OSL decay of Al_2O_3:C at various values of dose.

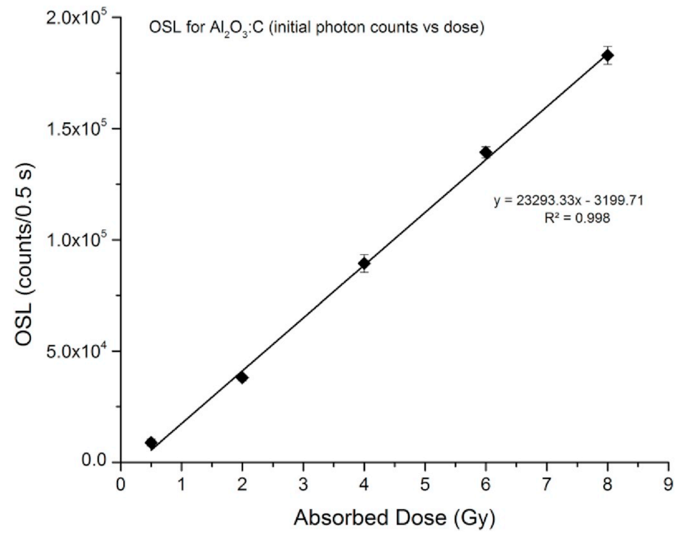

Fig. 4. Dose linearity of Al_2O_3:C using initial intensities.

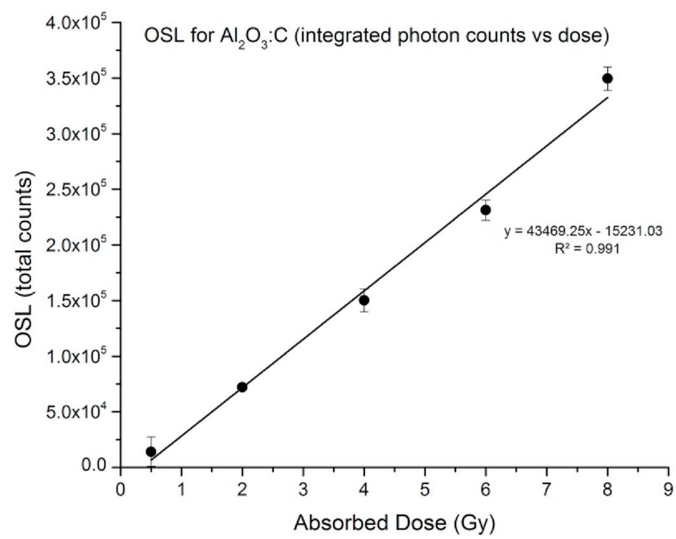

Fig. 5. Dose linearity of Al_2O_3:C using integrated photon counts.

monitoring the luminescence emission. Although the stimulation is pulsed, the OSL monitored is CW-OSL, thus the possibility exists that the optical stimulation may be greater than the lifetime of the intrinsic luminescence emission from the dosimeter. The repetition frequency may thus be limited, a matter beyond the scope of present work with dependence being on the detector medium rather than the reader.

3.3. *Dose response linearity of Al_2O_3:C*

Fig. 3 shows the CW-OSL signal shapes from Al_2O_3:C at a number of arbitrary dose points, 0.5-, 2-, 4-, 6- and 8 Gy, a range encompassing values familiarly used in the conduct of fractionated external beam radiotherapy. Post stimulation of the sample, data has been recorded for a read time of some 10.5 s. The shape of the curves follows the typical CW-OSL response, albeit with the OSL signal decay becoming more acute with increase in dose. The decay rate results from the combined effect of dose and defect depth dependency, greater rates of detrapping resulting from the more superficial traps; the latter are preferentially filled at lower dose. This accords with the interpretation of McKeever (2001), the CW-OSL decay curve shape being said to be dependent on the sample and absorbed dose, also noting further dependencies upon the wavelength and intensity of the stimulation light, as well as upon temperature.

The dose response linearity can be assessed from two distinct approaches, either the initial OSL intensity or total photon counts, integrating with the OSL decay curve. A cautionary note concerns the fact that the initial OSL intensity is more vulnerable to fluctuations in stimulation power (Yukihara and McKeever, 2008), the statement being supported by noting the dependency on choice of signal at low dose ($<$ 1 Gy), with both initial intensity and the total OSL area (inclusive of phosphorescence) being shown to be proportional to absorbed dose. Of note is that as dose increases, the initial OSL intensity is supralinear, related to the changing shape of the OSL curve with dose. In regard to dosimetry, some commercial OSL readers allow the user to record the entire OSL curve, providing choice between use of the total OSL (with phosphorescence) signal or parts of the OSL curve (such as the initial intensity). Other types of reader stimulate dosimeters for a short period of time, the corresponding initial OSL intensity needing to be checked (Yukihara and McKeever, 2011).

In respect of initial OSL intensity and use of the prototype OSL reader, the dose response over the investigated dose range (0.5 Gy up to 8 Gy) was found to be highly linear, with R^2 of 0.998 (Fig. 4). Conversely the total OSL signal was less so, $R^2 = 0.991$ (Fig. 5), the total response being the sum of OSL and phosphorescence signals; the expectation is of a more supralinear response. The y-axis error bars represent the response range covered by five identical Al_2O_3:C OSL dosimeter readings at each dose. On the basis of present results and in support of clinical linac applications it is apparent that the present in-house prototype reader offers excellent and versatile OSL measurements performance.

4. Conclusions

Present work set out to design, construct and test a novel OSL reader, sufficient in versatility and capability to allow investigation of the performance of various OSL materials, also incorporating a fibre mounted sensor arrangement for stand-off (at a distance) measurements. An important challenge was the need to produce a device within the boundaries of a limited experimental budget, a budget far less than the cost of purchasing a commercially available system. Faced with this challenge, numerous methods were considered in seeking to reduce costs while also increasing flexibility, including the use of off-the-shelf optical components. One example was selection of relatively new, higher power LEDs, less elaborate than more conventional light sources, lasers or broad spectrum bulbs included, the latter requiring use of associated monochromators. Further integration of design features has allowed for simple and rapid changing of key system components. The completed device has been tested, demonstrating an ability to meet a range of essential goals including performance of a variety of CW-OSL and pulsed OSL functions. While many desirable enhancements and improvements are possible, the current design allows the use of excitation sources operating at wavelengths other than current commercial readers, also providing for the ability to swap out filters and other components to test a range of sensors and wavelength dependencies. It is hoped that the information contained herein will help others to pursue OSL experimentation in this exciting and important area of dosimetry research.

Acknowledgements

The project was carried out with support from grants University of Malaya, Ministry of Higher Education of Malaysia, UMMOHE, High Impact Research Grant UM.C/625/1/HIR/33 and Multimedia University, Malaysia Fundamental Research Grant Scheme FRGS/1/2012/SG02/MMU/02/2. Also acknowledged for the first and second authors are scholarships from the Bangladesh Government scheme “Bangabandhu Fellowship on Science and ICT Project” through the Ministry of Science and Technology Bangladesh.

Appendix A. Supplementary data

Supplementary data to this article can be found online at https://doi.org/10.1016/j.radphyschem.2019.108464.

References

Ahmed, M.F., Schnell, E., Ahmad, S., Yukihara, E.G., 2016. Image reconstruction algorithm for optically stimulated luminescence 2D dosimetry using laser-scanned Al2O3:C and Al2O3:C,Mg films. Phys. Med. Biol. 61 (20), 7484–7506.

Akselrod, M.S., Bøtter-Jensen, L., McKeever, S.W.S., 2007. Optically stimulated luminescence and its use in medical dosimetry. Radiat. Meas. 41, S78–S99.

Andersen, C.E., Nielsen, S.K., Greilich, S., Helt-Hansen, J., Lindegaard, J.C., Tanderup, K., 2009. Characterization of a fiber-coupled Al_2O_3:C luminescence dosimetry system for online in vivo dose verification during 192Ir brachytherapy. Med. Phys. 36, 708–718.

Aznar, M.C., Andersen, C.E., Bøtter-Jensen, L., Bäck, S.Å.J., Mattsson, S., Kjær-Kristoffersen, F., Medin, J., 2004. Real-time optical-fibre luminescence dosimetry for radiotherapy: physical characteristics and applications in photon beams. Phys. Med. Biol. 49, 1655–1669.

Barve, R., Patil, R.R., Gaikwad, N.P., Kulkarni, M.S., Mishra, D.R., Soni, A., Bhatt, B.C., Moharil, S.V., 2013. Optically stimulated luminescence and thermoluminescence in some Cu+ doped alkali fluoro-silicates. Radiat. Meas. 59, 73–80.

Bøtter-Jensen, L., McKeever, S.W., Wintle, A.G., 2003. Optically Stimulated Luminescence Dosimetry. Elsevier.

Gaza, R., McKeever, S.W.S., Akselrod, M., 2005. Near-real-time radiotherapy dosimetry using optically stimulated luminescence of Al_2O_3:C: mathematical models and preliminary results. Med. Phys. 32, 1094–1102.

Granville, D.A., Sahoo, N., Sawakuchi, G.O., 2014. Linear energy transfer dependence of Al2O3:C optically stimulated luminescence detectors exposed to therapeutic proton beams. Radiat. Meas. 71, 69–73.

Kerns, J.R., Kry, S.F., Sahoo, N., Followill, D.S., Ibbott, G.S., 2011. Angular dependence of the nanoDot OSL dosimeter. Med. Phys. 38 (7), 3955–3962.

Klein, D.M., Yukihara, E.G., Bulur, E., Durham, J.S., Akselrod, M.S., McKeever, S.W.S., 2005. An optical fiber radiation sensor for remote detection of radiological materials. IEEE Sens. J. 5 (4), 581–588.

Klein, D.M., Yukihara, McKeever, S.W.S., E., Durham, J.S., Akselrod, M.S., 2006. *In situ* long-term monitoring system for radioactive contaminants. Radiat. Prot. Dosim. 119, 421–424.

Marcazzó, J., Cruz-Zaragoza, E., Quang, V.X., Khaidukov, N.M., Santiago, M., 2011. OSL, RL and TL characterization of rare-earth ion doped K2YF5: application in dosimetry. J. Lumin. 131 (12), 2711–2715.

McKeever, S.W., 2001. Optically stimulated luminescence dosimetry. Nucl. Instrum. Methods Phys. Res. Sect. B Beam Interact. Mater. Atoms 184 (1), 29–54.

Mizanur Rahman, A.K.M., Begum, M., Begum, M., Zubair, H.T., Abdul-Rashid, H.A., Yusoff, Z., Bradley, D.A., 2018. Radioluminescence of Ge-doped silica optical fibre and Al_2O_3: C dosimeters. Sens. Actuators A Phys. 270, 72–78.

Mizanur Rahman, A.K.M., Begum, M., Zubair, H.T., Abdul-Rashid, H.A., Yusoff, Z., Ung, N.M., Bradley, D.A., 2017. Ge-doped silica optical fibres as RL/OSL dosimeters for radiotherapy dosimetry. Sens. Actuators A Phys. 264, 30–39.

Ponmalar, R., Manickam, R., Ganesh, K.M., Saminathan, S., Raman, A., Godson, H.F., 2017. Dosimetric characterization of optically stimulated luminescence dosimeter with therapeutic photon beams for use in clinical radiotherapy measurements. J. Cancer Res. Ther. 13 (2), 304.

Sommer, M., Jahn, A., Henniger, J., 2011. A new personal dosimetry system for H_P (10) and H_P (0.07) photon dose based on OSL-dosimetry of beryllium oxide. Radiat. Meas. 46 (12), 1818–1821.

Wesolowska, P.E., Cole, A., Santos, T., Bokulic, T., Kazantsev, P., Izewska, J., 2017. Characterization of three solid state dosimetry systems for use in high energy photon dosimetry audits in radiotherapy. Radiat. Meas. 106, 556–562.

Yukihara, E.G., McKeever, S.W., 2011. Optically Stimulated Luminescence: Fundamentals and Applications. John Wiley & Sons.

Yukihara, E.G., McKeever, S.W.S., 2008. Optically stimulated luminescence (OSL) dosimetry in medicine. Phys. Med. Biol. 53 (20), R351.

Yukihara, E.G., McKeever, S.W., Akselrod, M.S., 2014. State of art: optically stimulated luminescence dosimetry–frontiers of future research. Radiat. Meas. 71, 15–24.

Yukihara, E.G., Whitley, V.H., McKeever, S.W.S., Akselrod, A.E., Akselrod, M.S., 2004. Effect of high-dose irradiation on the optically stimulated luminescence of Al_2O_3:C. Radiat. Meas. 38 (3), 317–330.

Yusuf, M., Alothmany, N., Kinsara, A.A., 2017. Organ dose measurement using optically stimulated luminescence detector (OSLD) during CT examination. Radiat. Phys. Chem. 139, 83–89.